Formation and Characterization of the Oxygen-Rich Hafnium Dioxygen Complexes: $OHf(\eta^2\text{-}O_2)(\eta^2\text{-}O_3)$, $Hf(\eta^2\text{-}O_2)_3$, and $Hf(\eta^2\text{-}O_2)_4$

Yu Gong and Mingfei Zhou*

Department of Chemistry, Shanghai Key Laboratory of Molecular Catalysts and Innovative Materials, Advanced Materials Laboratory, Fudan University, Shanghai 200433, People's Republic of China

Received: June 12, 2007

Hafnium atom oxidation by dioxygen molecules has been investigated using matrix isolation infrared absorption spectroscopy. The ground-state hafnium atom inserts into dioxygen to form primarily the previously characterized HfO_2 molecule in solid argon. Annealing allows the dioxygen molecules to diffuse and react with HfO_2 to form $OHf(\eta^2\text{-}O_2)(\eta^2\text{-}O_3)$, which is characterized as a side-on bonded oxo−superoxo hafnium ozonide complex. Under visible light (532 nm) irradiation, the $OHf(\eta^2\text{-}O_2)(\eta^2\text{-}O_3)$ complex either photochemically rearranges to a more stable $Hf(\eta^2\text{-}O_2)_3$ isomer, a side-on bonded di-superoxo hafnium peroxide complex, or reacts with dioxygen to form an unprecedented homoleptic tetra-superoxo hafnium complex: $Hf(\eta^2\text{-}O_2)_4$. The $Hf(\eta^2\text{-}O_2)_4$ complex is determined to possess a D_{2d} geometry with a tetrahedral arrangement of four side-on bonded O_2 ligands around the hafnium atom, which thus presents an 8-fold coordination. These oxygen-rich complexes are photoreversible; that is, formation of $Hf(\eta^2\text{-}O_2)_3$ and $Hf(\eta^2\text{-}O_2)_4$ is accompanied by demise of $OHf(\eta^2\text{-}O_2)(\eta^2\text{-}O_3)$ under visible (532 nm) light irradiation and vice versa with UV (266 nm) light irradiation.

Introduction

The coordination of dioxygen to transition metal centers and its activation are of great interest in biological and catalytic systems. Great effort has been devoted to characterize the structures and reactivity of transition metal−dioxygen complexes, which are important reactive intermediates in most oxidation processes.[1−8] On the basis of the O−O bond distance and O−O stretching vibrational frequency, metal−dioxygen complexes have been defined as superoxo or peroxo complexes.[9] The chemistry of early transition metals with dioxygen is replete with the formation of high-valent oxo (O^{2-}) or peroxo (O_2^{2-}) compounds;[10−32] reports of superoxo complexes are rare.[33] A series of gas-phase investigations were limited to the neutral and ionic metal oxide clusters with different metal/O ratios.[10−18] Gas-phase kinetic[19−22] as well as matrix isolation spectroscopic studies[23−27] indicate that early transition metal atoms react with dioxygen directly to form metal oxides without a significant activation barrier. The binding of early transition metal complexes with dioxygen results in the formation of a number of heteroleptic transition metal peroxo complexes, which provide direct information about their structures and mechanisms of dioxygen activation.[28−31] Since the first preparation of $M_3[Ta(O_2)_4]$ (M = Na or K),[32] a large number of homoleptic tetraperoxometalate compounds of group V and VI metals have also been synthesized and characterized.[28−31] These compounds show the ability to release oxygen in active form, either by chemical means or under irradiation, and act in oxidations of inorganic and organic substrates.

Here we present a joint experimental and theoretical study of three oxygen-rich hafnium−dioxygen complexes, $OHf(\eta^2\text{-}O_2)(\eta^2\text{-}O_3)$, $Hf(\eta^2\text{-}O_2)_3$, and $Hf(\eta^2\text{-}O_2)_4$ produced via the reactions of hafnium atoms with dioxygen in solid argon. The $OHf(\eta^2\text{-}O_2)(\eta^2\text{-}O_3)$ molecule is characterized as an oxo−superoxo hafnium ozonide complex. It either photochemically rearranges to a more stable $Hf(\eta^2\text{-}O_2)_3$ isomer, a side-on bonded disuperoxo hafnium peroxide complex, or reacts with dioxygen to form an unprecedented tetra-superoxo hafnium complex: $Hf(\eta^2\text{-}O_2)_4$, which is determined to possess a D_{2d} geometry with a tetrahedral arrangement of four $\eta^2\text{-}O_2$ ligands around the hafnium atom with an 8-fold coordination.

Experimental and Theoretical Methods

The hafnium−dioxygen complexes were produced by the reactions of hafnium atoms with O_2 in solid argon. The experimental setup for pulsed laser evaporation and matrix isolation infrared spectroscopic investigation has been described in detail previously.[34] Briefly, the 1064 nm fundamental of a Nd:YAG laser (Continuum, Minilite II; 10 Hz repetition rate and 6 ns pulse width) was focused onto a rotating hafnium metal target through a hole in a CsI window cooled normally to 6 K by means of a closed-cycle helium refrigerator (ARS, 202N). The laser-evaporated hafnium atoms were co-deposited with O_2/Ar mixtures onto the CsI window. In general, matrix samples were deposited for 1−1.5 h at a rate of approximately 4 mmol/h. The O_2/Ar mixtures were prepared in a stainless steel vacuum line using standard manometric technique. O_2 (Shanghai BOC, >99.5%) and isotopic labeled $^{18}O_2$ (ISOTEC, 99%) were used without further purification. The infrared absorption spectra of the resulting samples were recorded on a Bruker IFS 66V spectrometer at 0.5 cm^{-1} resolution between 4000 and 400 cm^{-1} using a DTGS detector. Matrix samples were annealed at different temperatures. The second and forth harmonic output (532 and 266 nm) of a Nd:YAG laser (Spectra-Physics GCR150) was used for irradiation of selected samples with a repetition rate of 10 Hz and 6 ns pulse width.

Quantum chemical calculations were performed to determine the molecular structures and to help the assignment of vibrational

* To whom correspondence should be addressed. E-mail: mfzhou@fudan.edu.cn.

10.1021/jp074531m CCC: $37.00
Published on Web 08/24/2007

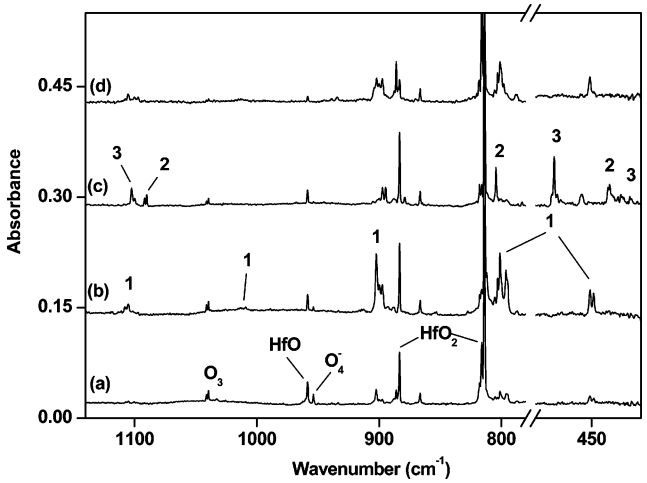

Figure 1. Infrared spectra in the 780−1140 and 415−490 cm^{-1} regions from co-deposition of laser-evaporated hafnium atoms with 0.25% O_2 in argon: (a) 1 h of sample deposition at 6 K, (b) after 35 K annealing, (c) after 45 min of 532 nm irradiation, and (d) after 15 min of 266 nm irradiation.

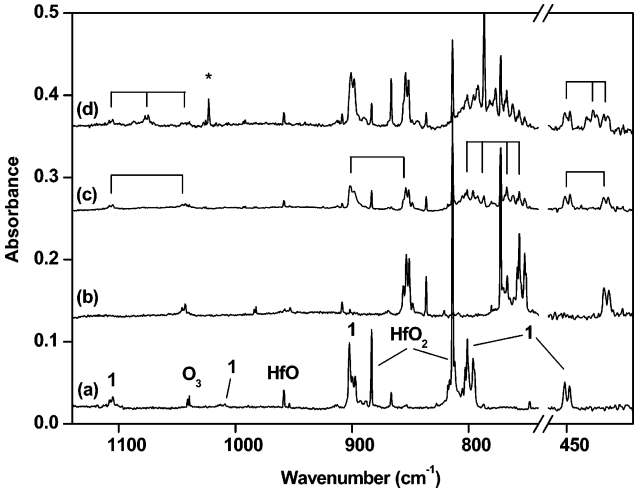

Figure 2. Infrared spectra in the 740−1140 and 415−460 cm^{-1} regions from co-deposition of laser-evaporated hafnium atoms with isotopic labeled O_2 in excess argon. Spectra were taken after 1 h of sample deposition followed by 35 K annealing: (a) 0.25% $^{16}O_2$, (b) 0.25% $^{18}O_2$, (c) 0.15% $^{16}O_2$ + 0.15% $^{18}O_2$, and (d) 0.1% $^{16}O_2$ + 0.2% $^{16}O^{18}O$ + 0.1% $^{18}O_2$. The asterisk denotes an impurity absorption from the mixed $^{16}O_2$ + $^{16}O^{18}O$ + $^{18}O_2$ sample.

frequencies of the observed reaction products. The calculations were performed at the level of density functional theory (DFT) with the B3LYP method, where Becke's three-parameter hybrid functional and the Lee−Yang−Parr correlation functional were used.[35] The 6-311+G(d) basis set was used for the O atom, and the scalar-relativistic SDD pseudopotential and basis set was used for the Hf atom.[36,37] Geometries were fully optimized, and vibrational frequencies were calculated with analytical second derivatives. These DFT calculations were performed using the Gaussian 03 program.[38]

Results and Discussion

Infrared Spectra. A series of experiments were performed with different O_2 concentrations (ranging from 0.05 to 2.0% in argon) and laser energies to control the relative concentrations of hafnium and O_2. With low O_2 concentration (0.05%) and high laser energy (12 mJ/pulse), the hafnium dioxide and monoxide absorptions were observed, which have been previously identified.[23] Dinulcear hafnium oxide clusters, Hf_2O_2 and Hf_2O_4, were produced on sample annealing.[39] When using relatively high O_2 concentrations (0.25−2.0%) and low laser energy (6−8 mJ/pulse), the hafnium monoxide and dioxide absorptions together with the known O_3 and O_4^- absorptions were observed after sample deposition,[40] but the dinuclear species were barely observed on sample annealing. By contrast, several new absorptions were produced upon sample annealing and photolysis, as illustrated in Figure 1. The observation of only under high O_2 concentration and low laser energy experimental condition implys that these new absorptions are due to mononuclear species. These new absorptions can be classified into three groups (labeled as 1, 2, and 3 in Figure 1) on the basis of their annealing and photochemical behaviors. The absorptions at 1105.6, 1014.3, 902.3, 801.3, 680.2, and 451.0 cm^{-1} (1) increased together on sample annealing. These absorptions almost disappeared upon 532 nm laser irradiation, during which the 1092.1, 1090.2, 804.4, 563.2, and 438.5 cm^{-1} absorptions (2) and 1102.4, 476.6, and 423.3 cm^{-1} absorptions (3) were produced. Additional irradiation with the 266 nm laser light destroyed group 2 and 3 absorptions and reproduced group 1 absorptions. Experiments with different O_2 concentrations (0.5, 1.0, and 2.0%) indicate that group **3** absorptions are favored relative to group **2** absorptions with high O_2 concentrations.

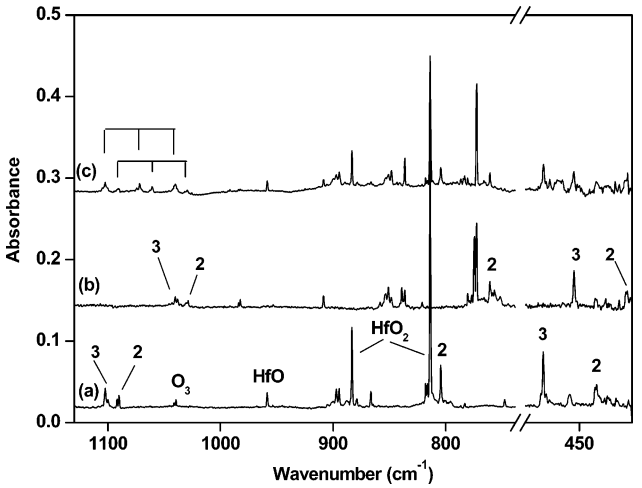

Figure 3. Infrared spectra in the 738−1130 and 410−490 cm^{-1} regions from co-deposition of laser-evaporated hafnium atoms with isotopic labeled samples in excess argon. Spectra were taken after sample deposition followed by 45 min of 532 nm irradiation: (a) 0.25% $^{16}O_2$, (b) 0.25% $^{18}O_2$, and (c) 0.15% $^{16}O_2$ + 0.15% $^{18}O_2$.

The experiments were repeated by using an isotopically labeled $^{18}O_2$ sample and the $^{16}O_2$ + $^{18}O_2$ and $^{16}O_2$ + $^{16}O^{18}O$ + $^{18}O_2$ mixtures. The spectra in selected regions with different isotopic samples are shown in Figures 2−4, respectively. The new product absorptions are summarized in Table 1.

OHf(η^2-O_2)(η^2-O_3). The absorptions at 1105.6, 1014.3, 902.3, 801.3, 680.2, and 451.0 cm^{-1} (1) were observed only in the experiments with relatively low laser energy and high O_2 concentrations, which suggests that only one hafnium atom is involved in this molecule. The 902.3 cm^{-1} absorption shifted to 856.0 cm^{-1} with $^{18}O_2$. The band position and $^{16}O/^{18}O$ isotopic frequency ratio (1.0541) imply that this band is due to a terminal Hf−O stretching vibration.[23,41] The spectra with the $^{16}O_2$ + $^{18}O_2$ and $^{16}O_2$ + $^{16}O^{18}O$ + $^{18}O_2$ mixtures (Figure 2, traces c and d) indicate that only one HfO fragment is involved in this mode. As listed in Table 1, the 1105.6, 1014.3, and 801.3 cm^{-1} absorptions all exhibit isotopic frequency shifts that are characteristic of O−O stretching vibrations. The 1105.6 cm^{-1} absorption splits into a doublet (1105.7 and 1043.6 cm^{-1}) in

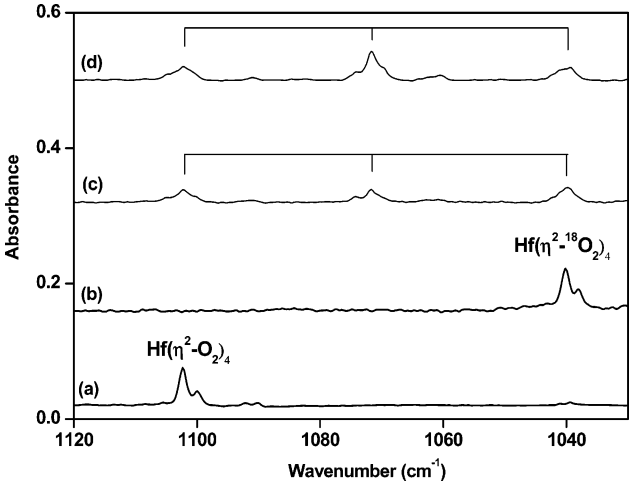

Figure 4. Infrared spectra in the 1030−1120 cm^{-1} region from co-deposition of laser-evaporated hafnium atoms with isotopic labeled samples in excess argon. Spectra were taken after sample deposition followed by 45 min of 532 nm irradiation: (a) 2.0% $^{16}O_2$, (b) 1.5% $^{18}O_2$, (c) 1.0% $^{16}O_2$ + 1.0% $^{18}O_2$, and (d) 0.5% $^{16}O_2$ + 1.0% $^{16}O^{18}O$ + 0.5% $^{18}O_2$.

the experiment with 1:1 mixtures of $^{16}O_2$ and $^{18}O_2$ (Figure 2, trace c) and a triplet positioned at 1105.7, 1075.1, and 1043.6 cm^{-1} in the experiment by using 1:2:1 mixtures of $^{16}O_2$, $^{16}O^{18}O$, and $^{18}O_2$ (Figure 2, trace d). These spectral features indicate that the molecule contains a side-on bonded O_2 subunit with two equivalent O atoms. The 451.0 cm^{-1} absorption is due to the Hf−O_2 stretching mode. The 801.3 cm^{-1} absorption splits into a quartet with approximately 1:1:1:1 relative IR intensities when the $^{16}O_2$ + $^{18}O_2$ sample was used (Figure 2, trace c). This quartet is about the same as that of the antisymmetric O−O stretching mode of O_3 observed at 1039.8 cm^{-1}, which suggests that species 1 also involves one O_3 subunit with two O atoms being equivalent. The 1014.3 and 680.2 cm^{-1} absorptions are much weaker than the 801.3 cm^{-1} absorption, and are due to the symmetric O−O stretching and O_3 bending modes of the O_3 subunit. According to the above-mentioned experimental observations, group 1 absorptions can be assigned to OHf(η^2-O_2)(η^2-O_3).

To validate the experimental assignment and to obtain insight into the structure and bonding of the complex, we performed density functional theory calculations of OHf(η^2-O_2)(η^2-O_3). The optimized geometry is shown in Figure 5. For the OHf(η^2-O_2)-(η^2-O_3) complex, a C_s structure in which the O_3 subunit and the central Hf atom lie in the same plane that is perpendicular to the molecular plane is considered. This C_s structure is a transition state based on the presence of a negative calculated frequency. The true minimum is only slightly distorted from the C_s symmetry. The side-on bonded O_2 fragment is due to a superoxide ligand with an O−O bond length of 1.332 Å.[9] The O_3 fragment also bound in a η^2 side-on fashion with two nearly equivalent Hf−O bond lengths of 2.229 and 2.252 Å, respectively. The distance between Hf and the central O atom of the O_3 fragment is 2.716 Å, suggesting no direct bonding interaction. The terminal Hf−O bond has a bond length of 1.777 Å, which can be regarded as a formal Hf−O triple bond.[42] Note that the experimentally observed antisymmetric O−O stretching vibration of the O_3 subunit is very close to that of the O_3^- anion isolated in solid argon.[43] Therefore, the OHf(η^2-O_2)(η^2-O_3) complex can be regarded as a side-on bonded oxo−superoxo hafnium ozonide complex, $[(HfO)^{2+}(O_2^-)(O_3^-)]$, that is, a HfO^{2+} dication coordinated by one O_2^- anion and one O_3^- anion. Bonding analysis indicates that the two unpaired electrons of the ^{3}A ground state OHf(η^2-O_2)(η^2-O_3) occupy the HOMO and HOMO-1 molecular orbitals, which are primarily antibonding π orbitals of the O_3 (LUMO b_1) and O_2 (SOMO π^*) subunits in character. The spin densities are mainly distributed at the O_2 (1.03 e) and O_3 (0.94 e) fragments. The natural population analyses indicate that Hf is positively charged with 2.32 e, while the O_2 and O_3 subunits are negatively charged with −0.64 e and −0.70 e, respectively.

The calculated vibrational frequencies and intensities for OHf-(η^2-O_2)(η^2-O_3) are listed in Table 2, and the isotopic frequency ratios are compared with the experimental values in Table 3. Six of seven modes in the spectral range of 400−4000 cm^{-1} were predicted to be IR active with appreciable intensities, which were experimentally detected with their frequencies and isotopic frequency ratios in good agreement with the experimental values, which add strong support to the experimental assignment. Recently, an analogous OTi(η^2-O_2)(η^2-O_3) complex was produced from the reaction of TiO_2 with O_2 in this laboratory, which was characterized to exhibit similar spectral and bonding properties as OHf(η^2-O_2)(η^2-O_3).[44]

Hf(η^2-O_2)$_3$. The absorptions at 1092.1, 1090.2, 804.4, 563.2, and 438.5 cm^{-1} (2) were produced under 532 nm laser irradiation, during which the OHf(η^2-O_2)(η^2-O_3) absorptions were destroyed. These absorptions are assigned to different vibrational modes of the Hf(η^2-O_2)$_3$ molecule, a structural isomer of the OHf(η^2-O_2)(η^2-O_3) complex. The 804.4 cm^{-1} absorption exhibits an O−O stretching vibrational $^{16}O/^{18}O$ ratio of 1.0574. The spectral feature in the mixed experiment (Figure 3, trace c) suggests the involvement of only one O_2 subunit in this mode. The band position indicates that this O_2 subunit is due to a peroxo ligand.[9] The 563.2 cm^{-1} absorption is the corresponding Hf−O_2 stretching mode of the peroxo subunit. The 1092.1 and 1090.2 cm^{-1} absorptions shifted to 1030.8 and 1028.8 cm^{-1} with $^{18}O_2$. The band positions and isotopic $^{16}O/^{18}O$ ratios of 1.0595 and 1.0597 are characteristic of the O−O stretching vibrations of superoxo ligands.[9] The 438.5 cm^{-1} absorption is the corresponding Hf−$(O_2)_2$ stretching mode of the superoxo fragments.

The experimental assignment is supported by DFT calculations. As shown in Figure 5, the Hf(η^2-O_2)$_3$ complex was predicted to have a ^{3}B ground state with C_2 symmetry. The Hf-(η^2-O_2)$_3$ complex is 6.1 kcal/mol more stable than the OHf(η^2-O_2)(η^2-O_3) isomer. At the optimized geometry of Hf(η^2-O_2)$_3$, two O_2 subunits are side-on bonded and are equivalent with an O−O bond length of 1.338 Å, which falls into the range of superoxide.[9] The third O_2 subunit is also side-on bonded with a much longer O−O bond length than that of the other two O_2 subunits. The predicted O−O bond length of 1.512 Å is appropriate for a peroxide complex.[9] Accordingly, the Hf(η^2-O_2)$_3$ molecule can be considered as $[Hf^{4+}(O_2^-)_2(O_2^{2-})]$, a side-on bonded di-superoxo hafnium peroxide complex. Consistent with this notion, the natural population analyses indicate that Hf is positively charged with 2.38 e, while the superoxo and peroxo ligands are negatively charged with −0.62 e and −1.14 e, respectively. The spin densities in the ^{3}B ground state of Hf-(η^2-O_2)$_3$ are mainly distributed at the two superoxo fragments (1.04 e each).

Hf(η^2-O_2)$_4$. Group 3 absorptions at 1102.4, 476.6, and 423.3 cm^{-1} appeared together with the Hf(η^2-O_2)$_3$ absorptions under 532 nm laser irradiation at the expense of OHf(η^2-O_2)(η^2-O_3). Hf(η^2-O_2)$_3$ is favored in the matrix for low O_2 concentrations, while species 3 dominates for high O_2 concentrations. The 1102.4 cm^{-1} absorption is due to an O−O stretching mode of superoxo ligands. The band positions and isotopic frequency

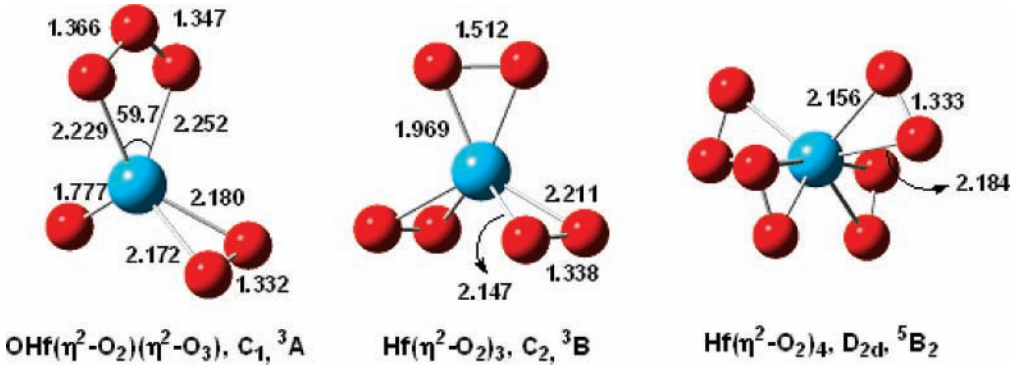

Figure 5. Optimized structures (bond lengths in angstrom, bond angles in degree) of the observed products.

TABLE 1: Product Absorptions (cm^{-1}) from the Reactions of Laser-Evaporated Hafnium Atoms with Dioxygen in Solid Argon

$^{16}O_2$	$^{18}O_2$	$^{16}O_2 + {}^{18}O_2$	$^{16}O_2 + {}^{16}O^{18}O + {}^{18}O_2$	assignment
1105.6	1043.6	1105.7, 1043.6	1105.7, 1075.1, 1043.6	OHf(η^2-O_2)(η^2-O_3) (O_2 stretch)
1108.3	1045.8	1108.2, 1045.8	1108.2, 1077.6, 1045.8	OHf(η^2-O_2)(η^2-O_3) site
1014.3	957.8			OHf(η^2-O_2)(η^2-O_3) (O_3 sym stretch)
1009.2	953.2			OHf(η^2-O_2)(η^2-O_3) site
902.3	856.0	901.9, 855.8	901.9, 855.8	OHf(η^2-O_2)(η^2-O_3) (Hf−O stretch)
899.9	853.4	901.0, 853.9	900.9, 854.1	OHf(η^2-O_2)(η^2-O_3) site
801.3	756.5	801.3, 792.0, 767.3, 756.5		OHf(η^2-O_2)(η^2-O_3) (O_3 asym stretch)
796.2	751.9	796.2, 786.9, 762.0, 751.9		OHf(η^2-O_2)(η^2-O_3) site
680.2	642.5			OHf(η^2-O_2)(η^2-O_3) (O_3 bending)
451.0	430.4	451.0, 430.7	451.0, 439.6, 430.7	OHf(η^2-O_2)(η^2-O_3) (Hf−O_2 stretch)
448.4	427.9	448.4, 428.1	448.4, 436.3, 428.4	OHf(η^2-O_2)(η^2-O_3) site
1092.1	1030.8			Hf(η^2-O_2)$_3$ (sym O_2 stretch)
1090.2	1028.8	1090.1,1060.7, 1029.6		Hf(η^2-O_2)$_3$ (asym O_2 stretch)
804.4	760.7	804.4, 783.2, 760.7		Hf(η^2-O_2)$_3$ (O_2 stretch)
563.2	534.6	563.4, 534.9		Hf(η^2-O_2)$_3$ (Hf−O_2 stretch)
438.5	415.6			Hf(η^2-O_2)$_3$ (Hf−$(O_2)_2$ stretch)
1102.4	1040.2	1102.2,1071.7, 1039.8	1102.2, 1071.7, 1039.8	Hf(η^2-O_2)$_4$ (O_2 stretch)
1099.0	1038.0			Hf(η^2-O_2)$_4$ (O_2 stretch)
476.6	453.9			Hf(η^2-O_2)$_4$ (Hf−O_2 stretch)
423.3				Hf(η^2-O_2)$_4$ (Hf−O_2 stretch)

TABLE 2: Calculated Total Energies (hartrees; after Zero Point Energy Corrections), Frequencies (cm^{-1}), and Intensities (km/mol) of the Products

molecule	energy	frequency (intensity)
OHf(η^2-O_2) (η^2-O_3) ^{3}A	−499.325054	1169.4(22), 1070.8(4), 899.9(137), 850.4(197), 688.0(27),456.2(17), 429.1(42),342.3(4),300.1(27), 241.2(5), 182.7(8), 180.3(13), 113.5(5), 86.1(3), 58.9(22)
Hf(η^2-O_2)$_3$ ^{3}B	−499.334622	1161.6(12), 1154.2(28), 841.5(80), 585.9(11), 567.5(45), 466.2(44), 465.2(8), 404.4(25), 399.6(18), 157.6(0), 133.7(10), 121.6(1), 104.1(10), 94.4(4), 56.1(23)
Hf(η^2-O_2)$_4$ $^5B_2$	−649.735660	1179.4(0), 1170.4(64), 1165.7(11), 488.9(1), 477.1(0), 449.6(132), 432.2(0), 406.0(17), 400.1(36), 155.1(0), 138.1(2), 129.5(0), 123.4(10), 103.4(18), 98.2(0), 91.6(0)

TABLE 3: Comparisons between the Calculated and Experimentally Observed Vibrational Frequencies (cm^{-1}) and Isotopic Frequency Ratios of the Products

		freq		$^{16}O/^{18}O$	
molecule	mode	calcd	obsd	calcd	obsd
OHf(η^2-O_2) (η^2-O_3) (^{3}A)	O_2 stretch	1169.4	1105.6	1.0608	1.0594
	O_3 sym stretch	1070.8	1014.3	1.0607	1.0590
	Hf−O stretch	899.9	902.3	1.0556	1.0541
	O_3 asym stretch	850.4	801.3	1.0607	1.0592
	O_3 bending	688.0	680.2	1.0604	1.0587
	Hf−O_2 stretch	429.1	451.0	1.0512	1.0479
Hf(η^2-O_2)$_3$ (^{3}B)	O_2 sym stretch (a)	1161.6	1092.1	1.0607	1.0595
	O_2 asym stretch (b)	1154.2	1090.2	1.0607	1.0597
	O_2 stretch (a)	841.5	804.4	1.0592	1.0574
	Hf−O_2 stretch (a)	567.5	563.2	1.0525	1.0535
	Hf−$(O_2)_2$ stretch (b)	466.2	438.5	1.0517	1.0551
Hf(η^2-O_2)$_4$ ($^5B_2$)	O_2 stretch (e)	1170.4	1102.4	1.0607	1.0598
	Hf−O_2 stretch (e)	449.6	476.6	1.0490	1.0500
	Hf−O_2 stretch (e)	400.1	423.3	1.0568	

ratios imply that the 476.6 and 423.3 cm^{-1} absorptions are due to Hf−O_2 stretching vibrations. No vibrational modes were observed in the terminal Hf−O stretching frequency region, suggesting that species 3 is most likely due to a homoleptic hafnium dioxygen complex. Thus, we assign absorber 3 to Hf(η^2-O_2)$_4$, which is, to the best of our knowledge, the first neutral homoleptic tetra-superoxo complex of transition metals. The Hf(η^2-O_2)$_4$ complex was computed to have a $^5B_2$ ground state with a D_{2d} geometry, in which four side-on bonded O_2 ligands are tetrahedrally arranged around the hafnium atom (Figure 5). The optimized D_{2d} structure is very similar to that of the previously characterized group V and VI tetraperoxometalate anions.[28−31] The complex was calculated to have strong O−O stretching and Hf−O_2 stretching vibrations at 1170.4 and 449.6 cm^{-1} (Table 2). The experiments with mixed $^{16}O_2 + {}^{18}O_2$ and $^{16}O_2 + {}^{16}O^{18}O + {}^{18}O_2$ samples (Figure 4) provide a conclusive method to identify this species. In the experiment with an equal molar mixture of $^{16}O_2$ and $^{18}O_2$, a triplet positioned at 1102.2, 1071.7, and 1039.8 cm^{-1} was observed. Note that the 1102.2 and 1039.8 cm^{-1} absorptions are broadened and the band centers

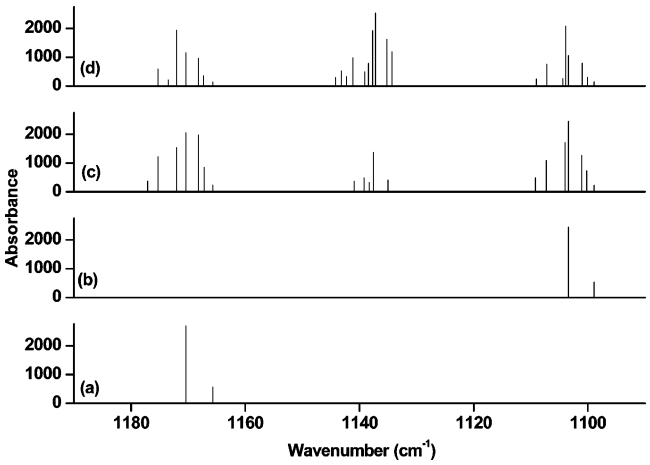

Figure 6. Simulated isotopic spectra of Hf(η^2-O_2)$_4$ in the O−O stretching frequency region: (a) $^{16}O_2$, (b) $^{18}O_2$, (c) $^{16}O_2 + {}^{18}O_2$ (1:1), and (d) $^{16}O_2 + {}^{16}O^{18}O + {}^{18}O_2$ (1:2:1).

are slightly shifted from the band centers (1102.4 and 1040.2 cm^{-1}) observed in the experiments using $^{16}O_2$ and $^{18}O_2$ separately. The IR intensity of the intermediate absorption at 1071.7 cm^{-1} is weaker than the 1102.2 and 1039.8 cm^{-1} absorptions. In the experiment when a 1:2:1 mixture of $^{16}O_2$, $^{16}O^{18}O$, and $^{18}O_2$ was used, the same absorptions were observed. However, the intermediate absorption at 1071.7 cm^{-1} is stronger than the 1102.2 and 1039.8 cm^{-1} absorptions. The experimentally observed spectra are in excellent agreement with the calculated isotopic spectral features shown in Figure 6, assuming that the Hf(η^2-O_2)$_4$ complex is formed from the reaction of OHf(η^2-O_2)(η^2-O_3) and O_2. The mixed isotopic features of the Hf−O_2 stretching modes of the Hf(η^2-O_2)$_4$ complex cannot be resolved due to isotopic dilution.

The O−O bond length in each O_2 fragment of Hf(η^2-O_2)$_4$ was predicted to be 1.333 Å, very close to the value of 1.332 Å in the recently reported unperturbed superoxide ion.[45] The two oxygen atoms in each O_2 subunit are slightly inequivalent with Hf−O bond lengths of 2.156 and 2.184 Å, respectively. The complex can be characterized as [$Hf^{4+}(O_2^-)_4$], that is, a side-on bonded tetra-superoxo hafnium complex. The $^5B_2$ ground state of Hf(η^2-O_2)$_4$ has an electronic configuration of (core)$(a_2)^1(b_1)^1(e)^2$ with two unpaired electrons occupying the nonbonding a_2 and b_1 molecular orbitals, which are linear combinations of four O_2^- π^* orbitals. The remaining two unpaired electrons occupy the doubly degenerate e molecular orbitals, which are also combinations of four O_2^- π^* orbitals but comprise significant O_2^- π^* to Hf^{4+} bonding. The natural population analysis shows that Hf is positively charged with 2.28 e, while each O_2 fragment is negatively charged with −0.57 e.

Recent matrix isolation investigation of thermally evaporated aluminum atoms with O_2 gave a series of aluminum dioxygen complexes.[46] The Al(η^2-O_2)$_3$ complex with D_3 symmetry was characterized to be a 6-fold coordinated superoxo complex, in which a Al^{3+} trication is coordinated by three superoxo O_2^- anions. The O−O and Al−O_2 stretching vibrational modes were observed at 1065 and 686 cm^{-1}, respectively. Compared to aluminum, which has only three valence electrons, hafnium has four valence electrons with the highest oxidation state of +4, and hence it is able to form 8-fold coordinated tetrasuperoxo complex.

Reaction Mechanism. The behavior of the product absorptions leads us to propose the following reactions (Scheme 1):

SCHEME 1

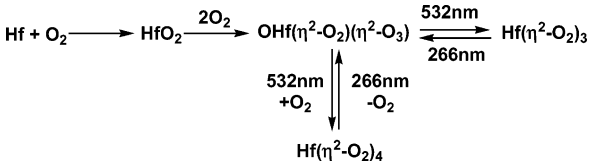

Laser-evaporated hafnium atoms reacted with O_2 to form the hafnium dioxide molecules. This insertion reaction is highly exothermic and proceeds without activation energy.[23] Annealing the matrix sample allows the O_2 molecules to diffuse and react with HfO_2 to form the OHf(η^2-O_2)(η^2-O_3) complex. This process was predicted to be exothermic by 44.1 kcal/mol. The OHf-(η^2-O_2)(η^2-O_3) complex absorptions increased on annealing, which suggests that this reaction requires negligible activation energy.

Under 532 nm laser irradiation, the OHf(η^2-O_2)(η^2-O_3) absorptions disappeared, during which the Hf(η^2-O_2)$_3$ absorptions were produced. This observation suggests that the OHf(η^2-O_2)(η^2-O_3) complex undergoes photoinduced isomerization to Hf(η^2-O_2)$_3$. According to the DFT calculations, the triplet ground state of Hf(η^2-O_2)$_3$ is 6.0 kcal/mol lower in energy than the triplet ground state OHf(η^2-O_2)(η^2-O_3) isomer. Hence, this isomerization reaction is exothermic but requires activation energy. The barrier height was computed to be 24.9 kcal/mol. The isomerization process proceeds only under visible light (532 nm) irradiation, during which some excited states may be involved. The HfO molecule has a high density of allowed transitions in the visible region for excitation of the metal monoxide in the OHf(η^2-O_2)(η^2-O_3) complex.[47]

The absorptions due to the Hf(η^2-O_2)$_4$ complex also were produced upon 532 nm laser irradiation with high O_2 concentrations. It appears that Hf(η^2-O_2)$_4$ is formed by the reaction of OHf(η^2-O_2)(η^2-O_3) and O_2, which was predicted to be exothermic by 27.7 kcal/mol. The reaction may proceed via the initial formation of an OHf(η^2-O_2)(η^2-O_3)(η^1-OO) complex, which was predicted to be weakly bound with respect to OHf(η^2-O_2)(η^2-O_3) and O_2. The infrared absorptions of the complex were computed to be only slightly shifted from those of OHf(η^2-O_2)(η^2-O_3), and cannot be resolved from the OHf(η^2-O_2)(η^2-O_3) absorptions in the experiments.

It is notable that the OHf(η^2-O_2)(η^2-O_3) absorptions partially recovered under 266 nm laser irradiation, during which the Hf-(η^2-O_2)$_3$ and Hf(η^2-O_2)$_4$ absorptions were bleached. These experimental observations indicate that the above characterized hafnium−dioxygen complexes are photoreversible; that is, formation of Hf(η^2-O_2)$_3$ and Hf(η^2-O_2)$_4$ is accompanied by demise of OHf(η^2-O_2)(η^2-O_3) under visible (532 nm) light irradiation, and vice versa with UV (266 nm) light irradiation. Photoreversible reactions have recently been reported for some transition metal methylidene systems.[48] The ability to release oxygen upon irradiation suggests that Hf(η^2-O_2)$_4$ also may be active in oxidation of inorganic and organic substrates as that of the homoleptic tetraperoxometalate compounds of group V and VI metals.[28−31]

The photochemical reaction feature of OHf(η^2-O_2)(η^2-O_3) is different from that of OTi(η^2-O_2)(η^2-O_3) as recently reported in this group.[44] The OTi(η^2-O_2)(η^2-O_3) complex rearranges to the OTi(η^2-O_2)(η^1-O_3) isomer instead of forming the Ti(η^2-O_2)$_3$ and Ti(η^2-O_2)$_4$ complexes under visible light irradiation. The smaller atomic radius of titanium compared to that of hafnium generally restricts titanium to form high-fold coordinated complexes.

The present experimental and theoretical results demonstrate that the oxidation of hafnium atoms with dioxygen proceeds with the initial formation of hafnium dioxide molecules. At the experiments with excess dioxygen, the HfO_2 molecules further react with dioxygen to form the hafnium oxide complex, OHf-(η^2-O_2)(η^2-O_3), which can be converted to the homoleptic hafnium dioxygen complexes. The HfO_2, OHf(η^2-O_2)(η^2-O_3), Hf(η^2-O_2)$_3$, and Hf(η^2-O_2)$_4$ species all are high-valent compounds with hafnium in its formal +4 oxidation state. The present investigation also demonstrates that the reactions from 2-fold coordinated HfO_2 to 5-fold coordinated OHf(η^2-O_2)(η^2-O_3), and to 6-fold coordinated Hf(η^2-O_2)$_3$, and finally to 8-fold coordinated Hf(η^2-O_2)$_4$ are energetically favorable with increasing coordination numbers at the same oxidation state for hafnium.

Conclusions

The reactions of hafnium atoms with dioxygen at high O_2 concentrations have been investigated using matrix isolation infrared absorption spectroscopy. The ground-state hafnium atoms generated by laser evaporation react with dioxygen to form the previously characterized HfO_2 molecules in solid argon. At the experiments with excess dioxygen, the HfO_2 molecules further react with O_2 to form the OHf(η^2-O_2)(η^2-O_3) complex, a side-on bonded oxo−superoxo hafnium ozonide complex. Under visible light (532 nm) irradiation, the OHf(η^2-O_2)(η^2-O_3) complex either photochemically rearranges to a more stable Hf(η^2-O_2)$_3$ isomer, a side-on bonded di-superoxo hafnium peroxide complex, or reacts with dioxygen to form an unprecedented homoleptic tetrasuperoxo hafnium complex: Hf(η^2-O_2)$_4$. The Hf(η^2-O_2)$_4$ complex is determined to possess a D_{2d} geometry with a tetrahedral arrangement of four side-on bonded O_2 ligands around the hafnium atom, which thus presents an 8-fold coordination. The experimental observations indicate that the above characterized hafnium−dioxygen complexes are photoreversible; that is, formation of Hf(η^2-O_2)$_3$ and Hf(η^2-O_2)$_4$ is accompanied by demise of OHf(η^2-O_2)(η^2-O_3) under visible (532 nm) light irradiation, and vice versa with UV (266 nm) light irradiation. These oxygen-rich complexes are potential important intermediates in transition metal oxidations. The present investigation provides a model system in demonstrating the intrinsic mechanism of transition metal oxidations at molecular level under high O_2 concentrations.

Acknowledgment. This work is supported by NKBRSF (Grant 2007CB815203) and NNSFC (Grant 20433080) of China.

References and Notes

(1) (a) Maiti, D.; Fry, H. C.; Woertink, J. S.; Vance, M. A.; Solomon, E. I.; Karlin, K. D. *J. Am. Chem. Soc.* **2007**, *129*, 265. (b) Sarangi, R.; Aboelella, N.; Fujisawa, K.; Tolman, W. B.; Hedman, B.; Hodgson, K. O.; Solomon, E. I. *J. Am. Chem. Soc.* **2006**, *128*, 8286. (c) Lewis, E. A.; Tolman, W. B. *Chem. Rev.* **2004**, *104*, 1047. (d) Mirica, L. M.; Ottenwaelder, X.; Stack, D. T. P. *Chem. Rev.* **2004**, *104*, 1013.

(2) (a) Kryatov, S. V.; Rybak-Akimova, E. V.; Schindler, S. *Chem. Rev.* **2005**, *105*, 2175. (b) Momenteau, M.; Reed, C. A. *Chem. Rev.* **1994**, *94*, 659. (c) Kovaleva, E. G.; Neibergall, M. B.; Chakrabarty, S.; Lipscomb, J. D. *Acc. Chem. Res.* **2007**, *40*, 475.

(3) (a) Kieber-Emmons, M. T.; Annaraj, J.; Seo, M. S.; Van Heuvelen, K. M.; Tosha, T.; Kitagawa, T.; Brunold, T. C.; Nam, W.; Riordan, C. G. *J. Am. Chem. Soc.* **2006**, *128*, 14230. (b) Fujita, K.; Schenker, R.; Gu, W.; Brunold, T. C.; Cramer, S. P.; Riordan, C. G. *Inorg. Chem.* **2004**, *43*, 3324.

(4) (a) Smirnov, V. V.; Brinkley, D. W.; Lanci, M. P.; Karlin, K. D.; Roth, J. P. *J. Mol. Catal. A: Chem.* **2006**, *251*, 100. (b) Lanci, M. P.; Brinkley, D. W.; Stone, K. L.; Smirnov, V. V.; Roth, J. P. *Angew. Chem., Int. Ed.* **2005**, *44*, 7273.

(5) Bakac, A. *Adv. Inorg. Chem*. **2004**, *55*, 1.

(6) Girerd, J. J.; Banse, F.; Simaan, A. J. In *Metal-Oxo and Metal-Peroxo Species in Catalytic Oxidations*; Meunier, B., Ed.; Springer: Berlin, 2000; Vol. 97, p 145.

(7) Solomon, E. I.; Tuczek, F.; Root, D. E.; Brown, C. A. *Chem. Rev.* **1994**, *94*, 827.

(8) Pecoraro, V. L.; Baldwin, M. J.; Gelasco, A. *Chem. Rev.* **1994**, *94*, 807.

(9) (a) Cramer, C. J.; Tolman, W. B.; Theopold, K. H.; Rheingold, A. L. *Proc. Natl. Acad. Sci. U.S.A.* **2003**, *100*, 3635. (b) Hill, H. A. O.; Tew, D. G. In *Comprehensive Coordination Chemistry*; Wilkinson, G., Gillard, R. D., McCleverty, J. A., Eds.; Pergamon: Oxford, U.K., 1987; Vol. 2, p 315. (c) Vaska, L. *Acc. Chem. Res.* **1976**, *9*, 175. (d) Valentine, J. S. *Chem. Rev.* **1973**, *73*, 235.

(10) (a) Zhai, H. J.; Wang, L. S. *J. Am. Chem. Soc.* **2007**, *129*, 3022. (b) Zhai, H. J.; Wang, L. S. *J. Chem. Phys.* **2006**, *125*, 164315. (c) Huang, X.; Zhai, H. J.; Li, J.; Wang, L. S. *J. Phys. Chem. A* **2006**, *110*, 85. (d) Zhai, H. J.; Huang, X.; Cui, L. F.; Li, X.; Li, J.; Wang, L. S. *J. Phys. Chem. A* **2005**, *109*, 6019. (e) Gutsev, G. L.; Jena, P.; Zhai, H. J.; Wang, L. S. *J. Chem. Phys.* **2001**, *115*, 7935. (f) Wu, H. B.; Wang, L. S. *J. Chem. Phys.* **1998**, *108*, 5310.

(11) (a) Dong, F.; Heinbuch, S.; He, S. G.; Xie, Y.; Rocca, J. J.; Bernstein, E. R. *J. Chem. Phys.* **2006**, *125*, 164318. (b) Matsuda, Y.; Bernstein, E. R. *J. Phys. Chem. A* **2005**, *109*, 314. (c) Matsuda, Y.; Bernstein, E. R. *J. Phys. Chem. A* **2005**, *109*, 3803. (d) Matsuda, Y.; Shin, D. N.; Bernstein, E. R. *J. Chem. Phys.* **2004**, *120*, 4142. (e) Foltin, M.; Stueber, G. J.; Bernstein. E. R. *J. Chem. Phys.* **2001**, *114*, 8971.

(12) (a) Demyk, K.; van Heijnsbergen, D.; von Helden, G.; Meijer, G. *Astron. Astrophys.* **2004**, *420*, 547. (b) Asmis, K. R.; Meijer, G.; Bruemmer, M.; Kaposta, C.; Santambrogio, G.; Woeste, L.; Sauer, J. *J. Chem. Phys.* **2004**, *120*, 6461. (c) Fielicke, A.; Meijer, G.; von Helden. G. *J. Am. Chem. Soc.* **2003**, *125*, 3659. (d) von Helden, G.; Kirilyuk, A.; van Heijnsbergen, D.; Sartakov, B.; Duncan, M. A.; Meijer, G. *Chem. Phys.* **2000**, *262*, 31.

(13) (a) Zheng, W. J.; Bowen, K. H.; Li, J.; Dabkowska, I.; Gutowski, M. *J. Phys. Chem. A* **2005**, *109*, 11521. (b) Thomas, O. C.; Xu, S. J.; Lippa, T. P.; Bowen, K. H. *J. Cluster Sci.* **1999**, *10*, 525.

(14) (a) Engeser, M.; Weiske, T.; Schröder, D.; Schwarz, H. *J. Phys. Chem. A* **2003**, *107*, 2855. (b) Schröder, D.; Schwarz, H.; Shaik, S. *Struct. Bonding* **2000**, *97*, 91.

(15) (a) Sun, Q.; Rao, B. K.; Jena, P.; Stolcic, D.; Kim, Y. D.; Gantefor, G.; Castleman, A. W., Jr. *J. Chem. Phys*. **2004**, *121*, 9417. (b) Bell, R. C.; Zemski, K. A.; Justes, D. R.; Castleman, A. W., Jr. *J. Chem. Phys.* **2001**, *114*, 798. (c) Kooi, S. E.; Castleman, A. W., Jr. *J. Phys. Chem. A* **1999**, *103*, 5671.(d) Bell, R.C.; Zemski, K. A.; Kerns, K. P.; Deng, H. T.; Castleman, A. W., Jr. *J. Phys. Chem. A* **1998**, *102*, 1733. (e) Deng, H. T.; Kerns, K. P.; Castleman, A. W., Jr. *J. Phys. Chem.* **1996**, *100*, 13386.

(16) (a) Molek, K. S.; Jaeger, T. D.; Duncan, M. A. *J. Chem. Phys.* **2005**, *123*, 144313. (b) Molek, K. S.; Jaeger, T. D.; Duncan, M. A. *J. Chem. Phys.* **2005**, *123*, 144313.

(17) (a) Tono, K.; Terasaki, A.; Ohta, T.; Kondow, T. *Phys. Rev. Lett.* **2003**, *90*, 133402. (b) Tono, K.; Terasaki, A.; Ohta, T.; Kondow, T. *J. Chem. Phys.* **2003**, *119*, 11221.

(18) (a) Wenthold, P. G.; Gunion, R. F.; Lineberger, W. C. *Chem. Phys. Lett.* **1996**, *258*, 101. (b) Wenthold, P. G.; Jonas, K. L.; Lineberger, W. C. *J. Chem. Phys.* **1997**, *106*, 9961. (c) Gunion, R. F.; Dixon-Warren, S. J.; Lineberger, W. C.; Morse, M. D. *J. Chem. Phys.* **1996**, *104*, 1765.

(19) (a) Campbell, M. L. *J. Chem. Soc., Faraday Trans.* **1998**, *94*, 1687. (b) McClean, R. E.; Campbell, M. L.; Kolsch, E. J. *J. Phys. Chem. A* **1997**, *101*, 3348. (c) Campbell, M. L.; Hooper, K. L. *J. Chem. Soc., Faraday Trans.* **1997**, *93*, 2139. (d) McClean, R. E.; Campbell, M. L.; Goodwin, Robert, H. *J. Phys. Chem. A* **1996**, *100*, 7502. (e) Campbell, M. L.; McClean, R. E.; Harter, J. S. S. *Chem. Phys. Lett.* **1995**, *235*, 497.

(20) (a) Ritter, D.; Weisshaar, J. C. *J. Phys. Chem.* **1989**, *93*, 1576. (b) Ritter, D.; Weisshaar, J. C. *J. Phys. Chem.* **1990**, *94*, 4907.

(21) (a) Haynes, C. L.; Honma, K. *J. Chem. Soc., Faraday Trans*. **1998**, *94*, 1171. (b) Honma, K. *J. Phys. Chem. A* **1999**, *103*, 1809. (c) Clemmer, D. E.; Honma, K.; Koyano, I. *J. Phys. Chem.* **1993**, *97*, 11480.

(22) Vetter, R.; Naulin, C.; Costes, M. *Phys. Chem. Chem. Phys.* **2000**, *2*, 643.

(23) Chertihin, G. V.; Andrews, L. *J. Phys. Chem.* **1995**, *99*, 6356.

(24) (a) Chertihin, G. V.; Bare, W. D.; Andrews, L. *J. Phys. Chem. A* **1997**, *101*, 5090. (b) Zhou, M. F.; Andrews, L. *J. Phys. Chem. A* **1998**, *102*, 8251. (c) Chertihin, G. V.; Bare, W. D.; Andrews, L. *J. Chem. Phys.* **1997**, *107*, 2798. (d) Bare, W. D.; Souter, P. F.; Andrews, L. *J. Phys. Chem. A* **1998**, *102*, 8279.

(25) (a) Brom, J. M., Jr.; Durham, C. H., Jr.; Weltner, W., Jr. *J. Chem. Phys*. **1974**, *61*, 970. (b) Hewett, W. D., Jr.; Newton, J. H.; Weltner, W., Jr. *J. Phys. Chem.* **1975**, *79*, 2640. (c) Weltner, W., Jr.; McLeod, D., Jr. *J. Mol. Spectrosc.* **1965**, *17*, 277.

(26) (a) Lorenz, M.; Bondybey, V. E. *Chem. Phys.* **1999**, *241*, 127. (b) Lorenz, M.; Agreiter, J.; Caspary, N.; Bondybey, V. E. *Chem. Phys. Lett.* **1998**, *291*, 291.

(27) Knight, L. B., Jr.; Babb, R.; Ray, M.; Banisaukas, T. J., III; Russon, L.; Dailey, R. S.; Davidson, E. R. *J. Chem. Phys.* **1996**, *105*, 10237.

(28) Butler, A.; Clague, M. J.; Meister, E. *Chem. Rev.* **1994**, *94*, 625.

(29) (a) Dickman, M. H.; Pope, M. T. *Chem. Rev.* **1994**, *94*, 569. (b) Bortolini, O.; Conte, V. *J. Inorg. Biochem.* **2005**, *99*, 1549. (c) Crans, D. C.; Smee, J. J.; Gaidamauskas, E.; Yang, L. Q. *Chem. Rev.* **2004**, *104*, 849.

(30) Sergienko, V. S. *Crystallogr. Rep.* **2004**, *49*, 1003.

(31) Bayot, D.; Devillers, M. *Coord. Chem. Rev.* **2006**, *250*, 2610.

(32) Balke, C. W. *J. Am. Chem. Soc.* **1905**, *27*, 1140.

(33) (a) Huang, X.; Zhai, H. J.; Waters, T.; Li, J.; Wang, L. S. *Angew. Chem., Int. Ed.* **2006**, *45*, 657. (b) Zhai, H. J.; Kiran, B.; Cui, L. F.; Li, X.; Dixon, D. A.; Wang, L. S. *J. Am. Chem. Soc.* **2004**, *126*, 16134. (c) Qin, K.; Incarvito, C. D.; Rheingold, A. L.; Theopold, K. H. *Angew. Chem., Int. Ed.* **2002**, *41*, 2333.(d) Almond, M. J.; Atkins, R. W. *J. Chem. Soc., Dalton Trans.* **1994**, 835.

(34) (a) Wang, G. J.; Gong, Y.; Chen, M. H.; Zhou, M. F. *J. Am. Chem. Soc.* **2006**, *128*, 5974. (b) Zhou, M. F.; Tsumori, N.; Xu, Q.; Kushto, G. P.; Andrews, L. *J. Am. Chem. Soc.* **2003**, *125*, 11371. (c) Zhou, M. F.; Andrews, L.; Bauschlicher, C. W., Jr. *Chem. Rev.* **2001**, *101*, 1931.

(35) (a) Becke, A. D. *J. Chem. Phys.* **1993**, *98*, 5648. (b) Lee, C.; Yang, W.; Parr, R. G. *Phys. Rev. B* **1988**, *37*, 785.

(36) (a) McLean, A. D.; Chandler, G. S. *J. Chem. Phys.* **1980**, *72*, 5639. (b) Krishnan, R.; Binkley, J. S.; Seeger, R.; Pople, J. A. *J. Chem. Phys.* **1980**, *72*, 650.

(37) (a) Dolg, M.; Stoll, H.; Preuss, H. *J. Chem. Phys.* **1989**, *90*, 1730. (b) Andrae, D.; Haussermann, U.; Dolg, M.; Stoll, H.; Preuss, H. *Theor. Chim. Acta* **1990**, *77*, 123.

(38) Frisch, M. J.; Trucks, G. W.; Schlegel, H. B.; Scuseria, G. E.; Robb, M. A.; Cheeseman, J. R.; Montgomery, J. A., Jr.; Vreven, T.; Kudin, K. N.; Burant, J. C.; Millam, J. M.; Iyengar, S. S.; Tomasi, J.; Barone, V.; Mennucci, B.; Cossi, M.; Scalmani, G.; Rega, N.; Petersson, G. A.; Nakatsuji, H.; Hada, M.; Ehara, M.; Toyota, K.; Fukuda, R.; Hasegawa, J.; Ishida, M.; Nakajima, T.; Honda, Y.; Kitao, O.; Nakai, H.; Klene, M.; Li, X.; Knox, J. E.; Hratchian, H. P.; Cross, J. B.; Adamo, C.; Jaramillo, J.; Gomperts, R.; Stratmann, R. E.; Yazyev, O.; Austin, A. J.; Cammi, R.; Pomelli, C.; Ochterski, J. W.; Ayala, P. Y.; Morokuma, K.; Voth, G. A.; Salvador, P.; Dannenberg, J. J.; Zakrzewski, V. G.; Dapprich, S.; Daniels, A. D.; Strain, M. C.; Farkas, O.; Malick, D. K.; Rabuck, A. D.; Raghavachari, K.; Foresman, J. B.; Ortiz, J. V.; Cui, Q.; Baboul, A. G.; Clifford, S.; Cioslowski, J.; Stefanov, B. B.; Liu, G.; Liashenko, A.; Piskorz, P.; Komaromi, I.; Martin, R. L.; Fox, D. J.; Keith, T.; Al-Laham, M. A.; Peng, C. Y.; Nanayakkara, A.; Challacombe, M.; Gill, P. M. W.; Johnson, B.; Chen, W.; Wong, M. W.; Gonzalez, C.; Pople, J. A. *Gaussian 03*, Revision B.05; Gaussian, Inc.: Pittsburgh, PA, 2003.

(39) Gong, Y.; Zhang, Q. Q.; Zhou, M. F. *J. Phys. Chem. A* **2007**, 111, 3534.

(40) Chertihin, G. V.; Andrews, L. *J. Chem. Phys.* **1998**, *108*, 6404.

(41) Zhou, M. F.; Zhang, L. N.; Dong, J.; Qin, Q. Z. *J. Am. Chem. Soc.* **2000**, *122*, 10680.

(42) (a) Gutsev, G. L.; Andrews, L.; Bauschlicher, C. W., Jr. *Theor. Chem. Acc.* **2003**, *109*, 298. (b) Siegbahn, P. E. M. *Chem. Phys. Lett.* **1993**, *201*, 15.

(43) (a) Andrews, L.; Ault, B. S.; Grzybowski, J. M.; Allen, R. O. *J. Chem. Phys.* **1975**, *62*, 2461. (b) Wight, C. A.; Ault, B., S.; Andrews, L. *J. Chem. Phys.* **1976**, *65*, 1244.

(44) Gong, Y.; Zhou, M. F.; Tian, S. X.; Yang, J. L. *J. Phys. Chem. A* **2007**, *111*, 6127.

(45) Dietzel, P. D. C.; Kremer, R. K.; Jansen, M. *J. Am. Chem. Soc.* **2004**, *126*, 4689.

(46) Stösser, G.; Schnöckel, H. *Angew. Chem., Int. Ed.* **2005**, *44*, 4261.

(47) Jonsson, J.; Edvinsson, G.; Taklif, A. G. *J. Mol. Spectrosc.* **1995**, *172*, 299.

(48) (a) Cho, H. G.; Andrews, L. *J. Am. Chem. Soc.* **2004**, *126*, 10485. (b) Andrews, L.; Cho, H. G. *Organometallics* **2006**, *25*, 4040.